Available online at www.sciencedirect.com
SCIENCE DIRECT
Geochimica et Cosmochimica Acta 70 (2006) 3351–3368
Geochimica
www.elsevier.com/locate/gca

Oil-generation kinetics for organic facies with Type-II and -IIS kerogen in the Menilite Shales of the Polish Carpathians

M.D. Lewan [a,*], M.J. Kotarba [b], J.B. Curtis [c], D. Więcław [b], P. Kosakowski [b]

[a] US Geological Survey, Box 25046, MS 977, Denver Federal Center, Denver, CO 80225, USA
[b] Faculty of Geology, Geophysics and Environmental Protection, University of Mining and Metallurgy, Al. Mickiewicza 30, 30-059 Krakow, Poland
[c] Department of Geology and Geological Engineering, Colorado School of Mines, Golden, CO 80401, USA

Received 3 August 2005; accepted in revised form 20 April 2006

Abstract

The Menilite Shales (Oligocene) of the Polish Carpathians are the source of low-sulfur oils in the thrust belt and some high-sulfur oils in the Carpathian Foredeep. These oil occurrences indicate that the high-sulfur oils in the Foredeep were generated and expelled before major thrusting and the low-sulfur oils in the thrust belt were generated and expelled during or after major thrusting. Two distinct organic facies have been observed in the Menilite Shales. One organic facies has a high clastic sediment input and contains Type-II kerogen. The other organic facies has a lower clastic sediment input and contains Type-IIS kerogen. Representative samples of both organic facies were used to determine kinetic parameters for immiscible oil generation by isothermal hydrous pyrolysis and S_2 generation by non-isothermal open-system pyrolysis. The derived kinetic parameters showed that timing of S_2 generation was not as different between the Type-IIS and -II kerogen based on open-system pyrolysis as compared with immiscible oil generation based on hydrous pyrolysis. Applying these kinetic parameters to a burial history in the Skole unit showed that some expelled oil would have been generated from the organic facies with Type-IIS kerogen before major thrusting with the hydrous-pyrolysis kinetic parameters but not with the open-system pyrolysis kinetic parameters. The inability of open-system pyrolysis to determine earlier petroleum generation from Type-IIS kerogen is attributed to the large polar-rich bitumen component in S_2 generation, rapid loss of sulfur free-radical initiators in the open system, and diminished radical selectivity and rate constant differences at higher temperatures. Hydrous-pyrolysis kinetic parameters are determined in the presence of water at lower temperatures in a closed system, which allows differentiation of bitumen and oil generation, interaction of free-radical initiators, greater radical selectivity, and more distinguishable rate constants as would occur during natural maturation. Kinetic parameters derived from hydrous pyrolysis show good correlations with one another (compensation effect) and kerogen organic-sulfur contents. These correlations allow for indirect determination of hydrous-pyrolysis kinetic parameters on the basis of the organic-sulfur mole fraction of an immature Type-II or -IIS kerogen.

1. Introduction

Source rocks in the Oligocene Menilite Shales have been shown to be responsible for petroleum accumulations in the Outer Flysch Carpathians of Poland (ten Haven et al., 1993). This structurally complex area consists of folded and thrusted strata of Cretaceous to late Miocene age. A series of imbricate nappe-thrust sheets extend north to northeast over strata of late Oligocene to Sarmatian age. Fig. 1 shows the location of the major nappe-thrust sheets that are referred to as "units" and are named from south to north as the Magura, Grybów, Dukla, Silesian, Skole, Stebnik, and Zglobice (Książkiewicz, 1977; Oszczypko, 1997). The northern-most thrust boundaries denote the start of the Carpathian Foredeep. Palinspastic reconstructions indicate the folding and thrusting reduced the original flysch basin by 31–58 percent (Nemčok et al., 2001). Variations in thickness and sedimentary facies of the flysch deposits within and among the major nappe-thrust sheets indicate subbasins

* Corresponding author. Fax: +1 303 236 3202.
E-mail address: mlewan@usgs.gov (M.D. Lewan).

0016-7037/$ - see front matter © 2006 Elsevier Inc. All rights reserved.
doi:10.1016/j.gca.2006.04.024

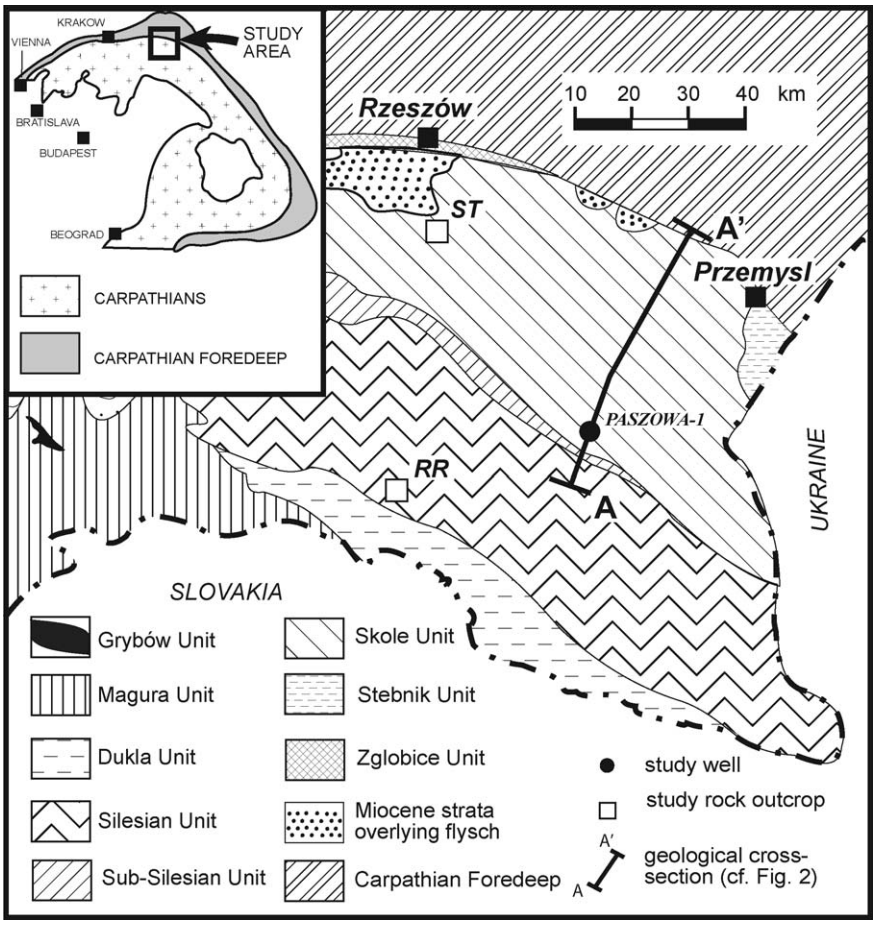

Fig. 1. Generalized geological map (modified after Książkiewicz, 1977 and Oszczypko, 1997) of the eastern Polish Carpathians showing the location of major tectonic units, sample sites, and cross-section.

existed during deposition of the Menilite Shales prior to late Miocene thrusting (Kuśmierek, 1996). These subbasins may have been separated by shallow or emergent paleo-highs developed during Late Cretaceous to Paleocene Laramide activity.

Within these subbasins, several organic facies of the Menilite source rocks have been recognized through the study of outcrop samples and crude oils (Curtis et al., 2004). Two of the recognized organic facies contain oil-prone kerogen and are differentiated by their organic-sulfur content, stable carbon isotopes, and biomarker constituents (Curtis et al., 2004). Samples of the high-sulfur organic facies are found in outcrops of the western part of the Skole unit (Fig. 1), where the exposed lower Menilite source rocks have less clastic input and a greater dominance of diatomaceous shale, diatomite, and chert (Kotlarczyk and Leśniak, 1990; Kuśmierek, 1996). Kerogen isolated from samples in this part of the section has atomic H/C, O/C, and S_{org}/C ratios indicative of Type-IIS kerogen (Curtis et al., 2004). Samples of the low-sulfur organic facies are found in the Silesian unit (Fig. 1), where the exposed Menilite source rocks have a greater clastic input characterized by argillaceous shale with interbedded sandstone. Kerogen isolated from samples in this part of the section has atomic H/C, O/C, and S_{org}/C ratios indicative of Type-II kerogen (Curtis et al., 2004).

Oils generated from these two organic facies are differentiated by their sulfur content (Curtis et al., 2004), with Type-IIS kerogen in the less clastic facies generating oils higher in sulfur than Type-II kerogen in the more clastic facies. The latter is considered to be responsible for the low-sulfur oil accumulations that are dominant in the nappe-thrust sheets, particularly the Silesian, and the former is considered to be responsible in part for the high-sulfur oil accumulations that are dominant in the Foredeep. Thickening of the section as a result of folding and thrusting was critical for Menilite source rocks to reach sufficient thermal maturities to generate petroleum in the thrust sheets (Bessereau et al., 1996). However, Foredeep oils that correlate to Menillite source rocks (ten Haven et al., 1993) indicate that these oils were generated prior to thrusting and have migrated long distances (Lafargue et al., 1994).

It has been reported that Type-IIS kerogen generates oil at considerably lower thermal maturities than Type-II kerogen as a result of labile sulfide bonds in the former initiating early free-radical cracking of carbon bonds (Lewan, 1998). The emerging scenario is that the organic facies with Type-IIS kerogen was responsible for early generation and

subsequent migration of high-sulfur oil into the Foredeep before major thrusting. The objective of this study is to test this scenario by determining kinetic parameters for oil-generation by laboratory pyrolysis of Menilite source rocks representing the two organic facies and evaluate them within the context of a pre-thrusting and thrusting burial history. Oil-generation kinetic parameters were determined using isothermal hydrous-pyrolysis and non-isothermal open-system pyrolysis.

2. Samples and methods

2.1. Description of samples

The two samples used in this study are from a larger collection of samples reported by Curtis et al. (2004). Table 1 gives analyses characterizing the rocks and their kerogen. Both rock samples have total organic carbon (TOC) contents in excess of 17 wt%. These samples contain Type-IIS and Type-II kerogen with minimal amounts of Type-III kerogen as indicated by their atomic elemental ratios (H/C, O/C, and S_{org}/C) and Rock-Eval hydrogen index (HI) and oxygen index (OI). Their T_{max}, mean random $\%R_o$, production index (PI), and atomic elemental ratios (H/C and O/C) indicate thermal immaturity.

Sample ST-4[u] was collected from a bank cut on the north side of the Lubenka Stream at the eastern end of Straszydle in the voivodeship of Fore-Carpathian (Fig. 1). The outcrop exposes Lower Menilite of the Łysa Gora anticline, which occurs on the south limb of the Błazowa-Przylaska syncline in the Skole thrust (Kotlarczyk and Leśniak, 1990). The outcrop consists of alternating beds of black diatomaceous shale, diatomite, and chert. The sample represents a 14-cm thick black diatomaceous shale near the base of the outcrop. Once the outer few centimeters of fissile shale were removed, a fresh slabby to blocky 10-kg sample with no saprolite rinds was collected in accordance with sampling criteria established by Lewan (1980). Petrographic analysis indicates the sample is shale with less than 25 vol% silt- to sand-sized quartz and some well-rounded glauconite grains. X-ray diffraction analysis and dilute HCl treatment indicate the sample contains clinoptilolite and 23 wt% calcite. According to Lewan (1978), this rock may be classified as a calcareous zeosiallitic claystone. As shown in Table 1, this sample contains Type-IIS kerogen with an organic-sulfur mole fraction (S_{org}/[S_{org} + C]) of 0.047.

Table 1
Description of Menilite samples

Sample designation	RR-45[2]	ST-4[u]
Kerogen analyses		
Classification	Type-II	Type-IIS
Atomic H/C ratio	1.29	1.43
Atomic O/C ratio	0.065	0.132
Atomic S_{org}/[C + S_{org}]	0.020	0.047
Mean random $\%R_o$	0.28	0.28
$\delta^{13}C$ (per mil, PDB)	−27.2	−28.0
Whole rock analyses		
TOC (wt%)	17.3	17.2
HI (mgS_2/gTOC)[a]	601	731
OI (mgS_3/gTOC)[a]	7	19
PI (S_1/[S_1 + S_2])[a]	0.03	0.03
T_{max} (°C)[a]	431	414

[a] Rock-Eval analyses.

Sample RR-45[2] was collected from an extensive Menilite outcrop in the Iwonicz Zdroj-Rudawka Rymanowska fold along the west bank of the Wisłok River between Pastwiska and Rudawka Rymanowska in the voivodeship of Fore-Carpathian (Fig. 1). This outcrop is in the Silesian unit where the Cergowa Sandstone member of the Lower Menilite Shales is exposed (Ślączka and Kamiński, 1998, p. 112). This member consists of sandstone with interbedded black siliceous shale. The sample represents an18-cm thick black siliceous shale about 3 m below a 0.5-m thick sandstone. Once the outer 25–35 cm of fissile and platy shale with jarosite coatings were removed, a fresh slabby to blocky 10-kg sample with no saprolite rinds was collected in accordance with sampling criteria established by Lewan (1980). Petrographic analysis indicates the sample is shale with less than 25 vol% silt- to sand-sized quartz and some well-rounded glauconite grains. X-ray diffraction analysis and dilute HCl treatment indicate the sample contains no zeolites and only 3 wt% carbonates. According to Lewan (1978), this rock may be classified as an argillaceous claystone. As shown in Table 1, this sample contains Type-II kerogen with an organic-sulfur mole fraction (S_{org}/[S_{org} + C]) of 0.020.

2.2. Isothermal hydrous pyrolysis

Rocks were crushed to gravel-sized chips (0.5–2 cm) and were not pre-extracted. An average bulk density was determined for the rock chips of both samples and used to calculate the amount of water needed to maintain liquid water in contact with the rock before, during, and after the experiments in 1-L reactors composed of 316-stainless steel or Hastelloy-C276 (Lewan, 1993). Hydrous pyrolysis of sample ST-4[u] required 350 g of rock and 360 g of distilled/deionized water and sample RR-45[2] required 300 g of rock and 360 g of distilled/deionized water. After loading and sealing the reactor, the remaining headspace was evacuated to less than 4 kPa and then filled with 7 MPa of helium. The pressurized reactor was checked for leaks using a thermal conductivity detector and then depressurized to a recorded helium pressure between 200 to 210 kPa. The reactor was then placed in an electric heater and brought to the desired experimental temperature within 0.83–1.16 h. The temperature was monitored and controlled by two J-type thermocouples in the thermal well of the reactor. Temperatures were recorded to 0.1 °C every 30 s from the turning on of the electric heaters to at least the first 10 h of cool down. Isothermal heating was conducted at temperatures between 300 and 365 °C with standard errors less than ±0.5 °C. Experimental times represent the duration

from the time the reactor gets within 0.5 °C of the desired experimental temperature during the warm up to the time the reactor falls below 0.5 °C of the desired experimental temperature after turning off the heater. Cool-down times range from 18 to 24 h.

As previously described (Lewan and Ruble, 2002), the hydrous-pyrolysis kinetic parameters are based on the generation of an expelled immiscible oil that is physically, chemically, and isotopically similar to natural crude oils. The generated expelled oil is immiscible with the water-saturated bitumen within the rock and as a result is expelled from the bitumen-impregnated rock as a separate immiscible oil phase (Lewan, 1997). Hydrous pyrolysis distinguishes between the initial thermal decomposition of insoluble kerogen to soluble polar-rich bitumen and the subsequent thermal decomposition of the polar-rich bitumen to immiscible hydrocarbon-rich oil (Lewan, 1985, 1993; Ruble et al., 2001). Increasing hydrous-pyrolysis temperatures on aliquots of an immature rock reveal these two overall sequential reactions by the initial decrease in kerogen content with a corresponding increase in bitumen content (i.e., kerogen to bitumen), followed by no change in the kerogen content with a decrease in bitumen content and a corresponding increase in the immiscible oil content (i.e., bitumen to oil). These two sequential overall reactions were originally recognized in oil-shale retorting studies (McKee and Lyder, 1921; Franks and Goodier, 1922; Maier and Zimmerley, 1924) and latter recognized in natural source-rock maturation studies (Louis and Tissot, 1967; Tissot, 1969). Bitumen generation from kerogen occurs at relatively low thermal-stress levels (<330 °C for 72 h) and calculated activation energies are typically less than 20 kcal/mol (e.g., Maier and Zimmerley, 1924; Braun and Rothman, 1975; Butler and Barker, 1986). Although more rigorous studies on types, mechanisms, and kinetics of bond cleavage in kerogen to form bitumen are needed (Miknis and Turner, 1995), the bonds are significantly weaker and more readily cleaved than covalent-bond cleavage responsible for oil generation from bitumen. This difference appears to be great enough that kerogen decomposition to bitumen is not a rate-controlling overall reaction in oil generation. As a result, hydrous-pyrolysis kinetic parameters derived in this study are for the overall reaction of bitumen to oil.

At the end of the experiments and following gas collection, the immiscible oil was quantitatively removed from the water surface in the reactor with a Pasteur pipette and a benzene rinse (Lewan, 1993). Immiscible oil is the sum of the expelled oil recovered by the pipette and benzene rinse. Previous studies have shown that variations in rock-chip size, water pH, water/rock ratios, and reactor-wall composition have no significant effect on the amount or composition of the generated immiscible oil (Lewan, 1993, 1997). These replicate experiments have a standard deviation of ±0.25 g for immiscible-oil yields between 5 and 14 g.

Two types of experiments were conducted; (1) temperature runs, and (2) time runs. Temperature runs consisted of 72-h experiments at 300, 310, 320, 330, 340, 350, 355, 360, and 365 °C. Results from these experiments were used to determine the character of an immiscible-oil curve, the maximum immiscible-oil yield for calculating transformation ratios (i.e., fraction of reaction), and the appropriate temperatures to use for the time runs. The time runs consist of isothermal experiments conducted at various times between 36 and 108 h at 320, 330, 340, and 350 °C. Results from these experiments were used to further evaluate maximum immiscible-oil yields and to determine rate constants at each of the time-series temperatures. The natural log of the resulting reaction-rate constants (k) was plotted against the reciprocal of their temperature in degrees Kelvin (K) to determine activation energy (E_a) from the slope and frequency factor (A_o) from the intercept of the Arrhenius equation:

$$\ln k = \ln A_o - E_a/RK, \tag{1}$$

where R is the ideal gas constant.

2.3. Non-isothermal open-system pyrolysis

Humble Geochemical Services conducted non-isothermal kinetic analyses with a SR Analyzer (Jarvie et al., 1996). Powdered aliquots of the two source-rock samples were pre-extracted with an azeotropic mixture of dichloromethane and methanol. The SR Analyzer initially heats 10- to 20-mg aliquots of the extracted powder for 5 min at 250 °C to remove existing volatile organic components (S_1 products) that may not have been removed by the pre-extraction step. Aliquots were then heated to 650 °C at heating rates of 1, 5, 15, 30, and 50 °C/min, with duplicate runs being made at 1 and 50 °C/min. For sample RR-45[2], three replicate runs at 50 °C/min were conducted. The alloy oven and electronics maintain a uniform temperature in the sample crucible with a standard error of ±1 °C. The organic components generated (i.e., S_2 products) during this non-isothermal heating are vaporized as a result of the low near-atmospheric pressures in the oven and are swept by a helium-carrier gas into a flame ionization detector (FID). The FID electronic response is calibrated with a hydrocarbon standard from which a quantitative yield is determined for the S_2 component.

Assuming the yield curves for each heating rate are a composite of parallel, first-order reactions with a common frequency factor, a discrete distribution of activation energies with a single frequency factor was computed by an iterative series of non-linear regression calculations. This computation assigns a fractional portion (x_i) of the overall yield to each prescribed activation-energy increment (E_{ai}). Increments of 1-kcal/mol were prescribed between 40 and 70 kcal/mol, and the frequency factor was unconstrained. These curve-fitting computations were made with the Kinetics2000 program. Specifics on these curve-fitting pro-

cedures and their development are given in Burnham and Braun (1999).

2.4. Burial history

The burial history used to evaluate the kinetic parameters determined in this study is from the Paszowa-1 well, which penetrates the Menilite Shales in the south-central part of the Skole unit (Fig. 2), which hosts low-sulfur oil accumulations derived from the Menilite Shales (ten Haven et al., 1993; Bessereau et al., 1996; Curtis et al., 2004). More than 95 wt% of this low-sulfur oil in the Skole unit occurs in the Kliwa Sandstone (Karnkowski, 1999, p. 76), which occurs within the Menilite Shales. The Skole unit is the first regionally extensive thrust sheet bordering the Carpathian Foredeep, which hosts some high-sulfur oils derived from the Menilite Shales (ten Haven et al., 1993; Bessereau et al., 1996; Curtis et al., 2004). According to isopach and paleostructure maps by Kuśmierek (1996), the Paszowa-1 well penetrates the Menilite Shales in a major Paleogene depocenter prior to major folding and thrusting. This location represents one of the deeper parts of the depocenter but not necessarily the deepest part.

The burial history for the Paszowa-1 well (Table 2) is based on thicknesses, uplifts, and erosion events determined by Kuśmierek and Maćkowski (1995) and Kuśmierek (1996). The thermal histories were reconstructed based on thermal parameters presented by Plewa (1976, 1991) and Majorowicz and Plewa (1979) that were calibrated with available vitrinite reflectance measurements and Rock-Eval T_{max} temperatures. The burial history given in Table 2 for this well includes three main stages responsible for the current Polish Carpathians. The first stage is sedimentation of Cretaceous through Middle Miocene flysch and molasse. Krosno and/or Transitional beds were deposited on the Menilite Shales between 26.5 and 23.2 Ma. This first stage ended with regional uplift and erosion designated as event A. The second stage represents the folding and northward thrusting of the sedimentary sequence onto itself, Precambrian or Paleozoic–Mesozoic basement, and part of the autochthonous Foredeep Miocene rocks (Ślączka, 1996; Oszczypko and Ślączka, 1989). This thrusting occurred over a distance of at least 40 km resulting in the major nappe-thrust units shown in Fig. 1 (Książkiewicz, 1977; Oszczypko, 1997). The third and final stage is post-inversion, which involves two periods of uplift and erosion designated as events B and C. Uplift and erosion event C represents the final overthrust of the orogenic belt on the autochthonous Miocene rocks of the Carpathian Foredeep (Oszczypko, 1997).

Timing of oil generation was determined for the base of the Menilite Shales. Organic facies with Type-IIS kerogen in the Menilite Shales have been documented with certainty in the northwestern part of the Skole unit (Curtis et al., 2004), and lithofacies maps by Kotlarczyk and Leśniak (1990) indicate that their chert facies thins to the southeast

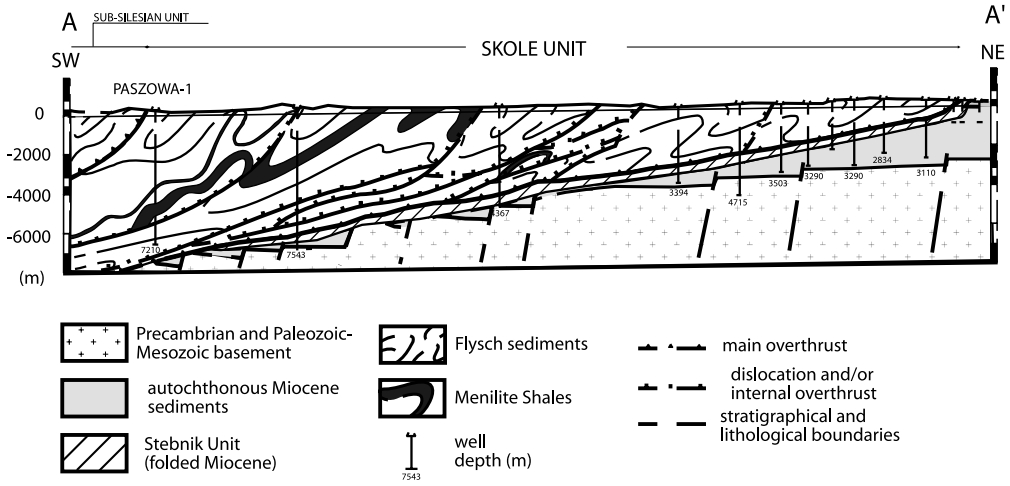

Fig. 2. Generalized cross-section of the Skole unit (modified after Cieszkowski et al., 1985 and Kruczek, 1999) and location of the Paszowa-1 well.

Table 2
Base of the Menilite Shales burial history in Paszowa-1 well

Geologic event	Thickness gained or lost (m)	Geologic age (Ma)	Thermal gradient (°C/km)	Surface temperature (°C)
Menilite Shale	580	33.7–26.5	37.5	11
Krosno + transitional	2280	26.5–23.2	33.0	10
Uplift/erosion A	−300	23.2–19.0	31.0	10
Folding + thrusting	2770	19.0–15.5	31.0	10
Uplift/erosion B	−170	15.5–10.8	25.5	9
Uplift/erosion C	−260	10.8–0.0	25.5	9

but does occur in the location of the Paszowa-1 well. Assuming their chert facies corresponds to the clastic-poor rocks with Type-IIS kerogen in the northwest, organic facies with Type-IIS and Type-II kerogen are considered in the burial history.

3. Results

3.1. Hydrous pyrolysis

Fig. 3 shows the product yields of bitumen, immiscible oil, and headspace gas for the temperature-series experiments at 72 h. As previously demonstrated (Lewan, 1985; Huizinga et al., 1988; Ruble et al., 2001), the bitumen yields increase during the initial stages of thermal maturation with apparent maximum yields occurring at 330 °C or less for 72-h experiments. Similar to previously reported results (Lewan, 1985), apparent maximum bitumen yield occurs at a lower temperature for Type-IIS kerogen (⩽300 °C) than for Type-II kerogen (Fig. 3). At or prior to these apparent maximum bitumen yields, the bitumen decomposes to immiscible oil that is expelled from the bitumen-impregnated rock. Gas generation monotonically increases with increasing thermal maturation with no abrupt changes associated with the start or end of bitumen or oil generation. Fig. 4 shows the distinct compositional differences between the polar-rich bitumen and the hydrocarbon-rich immiscible oil. These two distinct organic phases have been previously reported in hydrous-pyrolysis experiments and emphasize the importance of water in distinguishing kerogen decomposition to bitumen and bitumen decomposition to oil.

Yields of immiscible oil generated from samples ST-4[u] and RR-45[2] for all the experiments are, respectively, given in Tables 3 and 4 along with the experimental conditions. Maximum yields determined from these experiment are 347.8 mg/g TOC for ST-4[2] at 360 °C after 72 h and 324.3 mg/g TOC for RR-45[2] at 365 °C after 72 h. As demonstrated by Ruble et al. (2003), errors as high as 5 percent in determining the maximum yield of a source rock have a negligible effect on the resulting kinetic parameters. Concern that the maximum yields may be reduced by secondary cracking at the higher temperatures (i.e., 350–365 °C) is not significant as shown by the similarity in slope and distribution of the C_{24}–C_{30} *n*-alkanes in the immiscible oils generated at all of the temperatures for 72-h durations (Fig. 5). If significant cracking of the oil had occurred, the distributions would systematically loose their odd-carbon preference and steepen in slope as the higher alkanes are preferentially cracked with increasing experimental temperature. The lack of any abrupt changes in headspace gas generation (Fig. 3) or proportions of hydrocarbons and polars in the immiscible oils (Fig. 4) also indicate insignificant cracking of the immiscible oil at the higher temperatures.

The relation between maximum immiscible-oil yields from hydrous pyrolysis and the hydrogen index (HI; S_2/organic carbon) from open-system pyrolysis of the original unheated samples is in good agreement with published data

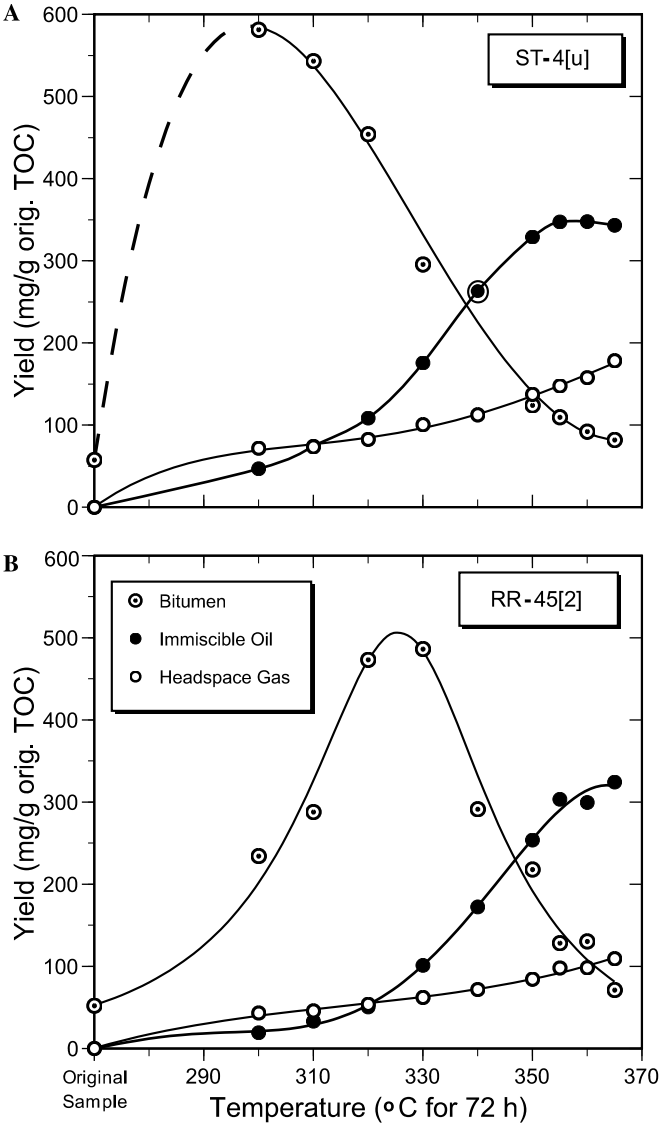

Fig. 3. Changes in hydrous-pyrolysis products generated at different temperatures (300–365 °C) for 72-h durations from samples (A) ST-4[u] and (B) RR-45[2]. Yields are calculated in milligrams of product per gram of original total organic carbon (TOC). General trend curves are best-fit polynomials with no theoretical basis. Bitumen yields were determined on pulverized (<0.2 mm) recovered rock (~10 g) that was extracted with a dichloromethane/methanol mixture (93:7 v/v) using a Soxtec apparatus. The extraction procedure consisted of a 2-h boiling followed by a 3-h rinse. Bitumens were concentrated by evaporation of the extracting solvent at ambient temperatures under a fume-hood until a constant weight was obtained. Generated gas yields are based on gas collected from reactor headspace and analyzed on a Wasson-Ece/Hewlett-Packard 6890 gas chromatograph using two thermal conductivity detectors and one flame ionization detector.

on other source rocks containing Type-II and -IIS kerogen (Fig. 6). This 2:1 relation is attributed to the higher concentration of polars (i.e., resins and asphaltenes) included in S_2 generated by open-system pyrolysis. Behar et al. (1997) have shown that 59 wt% of the S_2 generated by open-system pyrolysis consists of polars (Fig. 4), which by some definitions are considered to be non-hydrocarbons (e.g., Tissot and Welte, 1984, p. 180). Conversely, immiscible

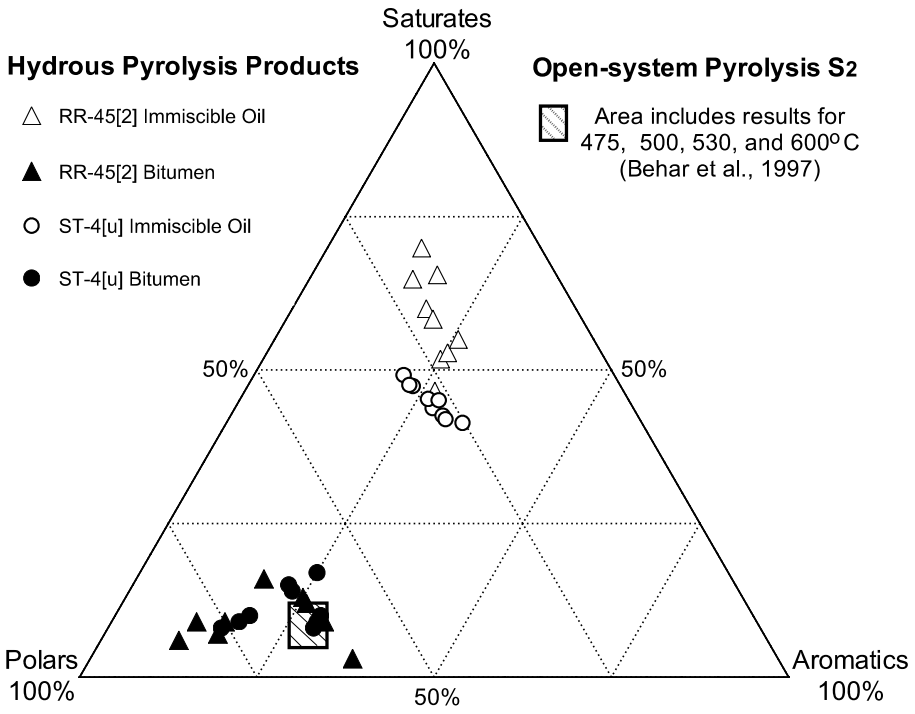

Fig. 4. Ternary diagram of C_{15+} saturate, aromatic, and polar (i.e., resins + asphaltenes) fractions of immiscible oils and bitumen generated by hydrous pyrolysis for 72-h durations at 300–365 °C for samples ST-4[u] and RR-45[2]. Saturate, aromatic, and resin fractions were determined by column chromatography using alumina/silica gel (2:1 v/v) columns (0.8 × 25 cm) and eluting solvents of hexane, benzene, and benzene: methanol (1:1 v/v), respectively. Asphaltenes were precipitated with *n*-hexane. The boxed field denotes compositions for S_2 products generated by open-system pyrolysis at 475, 500, 530, and 600 °C as reported by Behar et al. (1997).

Table 3
Hydrous pyrolysis conditions, immiscible oil yields, and decimal fraction of reaction for sample ST-4[u]

Series and experiment no.	Temperature (°C)	Warm-up time (h)	Temp. std. dev. (±°C)	Time (h)	Immiscible oil (mg/gTOC)	Fraction of reaction[a] (*X*)
Temperature series						
HP-2749	365.1	1.000	0.2	72.095	343.37	NA
HP-2751	360.1	1.008	0.5	72.136	**347.81**	1.0000
HP-2752	355.1	1.014	0.3	72.128	347.49	0.9991
HP-2754	350.1	0.978	0.2	72.099	328.99	0.9459
HP-2755	340.0	0.983	0.4	72.116	263.11	0.7565
HP-2767	329.8	0.958	0.5	72.091	175.73	0.5053
HP-2753	320.1	0.949	0.3	72.099	108.57	0.3122
HP-2750	310.0	0.971	0.2	72.053	74.40	0.2139
HP-2748	300.0	0.851	0.5	72.186	46.98	0.1351
Time series						
HP-2757	319.8	0.873	0.4	36.154	90.23	0.2594
HP-2762	320.1	1.041	0.2	108.128	151.45	0.4354
HP-2766	330.2	0.973	0.3	36.070	118.90	0.3419
HP-2761	330.0	0.972	0.3	108.120	187.61	0.5394
HP-2756	340.0	0.887	0.3	36.095	208.17	0.5985
HP-2764	340.0	0.908	0.2	108.120	287.94	0.8279
HP-2759	350.0	0.921	0.4	24.000	257.16	0.7394
HP-2758	350.1	0.966	0.3	48.100	314.73	0.9049

Maximum expelled-oil yield given in bold print. NA = not applicable.
[a] X = immiscible oil yield/347.81.

oil generated by hydrous pyrolysis contains between 15 and 25 wt% polars (Lewan, 1993; Ruble et al., 2001), which is closer to the 14–19 wt% average for natural crude oils (Tissot and Welte, 1984, p. 381). A particularly useful attribute of the relation in Fig. 6 is that hydrous-pyrolysis maximum immiscible-oil yields for rocks with Type-II and -IIS kerogen can be reasonably estimated from the Rock-Eval HI of the original immature rock.

Table 4
Hydrous pyrolysis conditions, immiscible oil yields, and decimal fraction of reaction for sample RR-45[2]

Series and experiment no.	Temperature (°C)	Warm-up time (h)	Temp. std. dev. (±°C)	Time (h)	Immiscible oil (mg/gTOC)	Fraction of reaction[a] (X)
Temperature series						
HP-2725	365.1	1.158	0.2	72.108	**324.30**	**1.000**
HP-2726	360.0	1.108	0.2	72.058	299.44	0.923
HP-2727	355.1	1.025	0.2	72.108	303.29	0.935
HP-2728	350.2	1.006	0.1	72.099	253.80	0.783
HP-2729	340.2	0.983	0.1	72.091	172.25	0.531
HP-2740	330.0	0.875	0.2	72.108	101.08	0.312
HP-2737	320.0	1.058	0.2	72.133	50.46	0.156
HP-2730	310.2	0.925	0.1	72.074	33.10	0.102
HP-2736	299.6	0.833	0.3	72.191	19.29	0.059
Time series						
HP-2742	320.2	1.020	0.2	36.029	35.65	0.110
HP-2734	320.0	0.916	0.2	108.078	78.30	0.241
HP-2741	330.4	0.908	0.6	36.087	61.08	0.188
HP-2735	330.0	0.958	0.3	108.186	135.88	0.419
HP-2744	340.2	1.029	0.3	36.104	94.41	0.291
HP-2738	340.0	1.066	0.2	108.095	217.57	0.671
HP-2733	350.1	1.007	0.2	36.104	179.50	0.553
HP-2739	350.0	0.975	0.3	108.037	268.61	0.828

Maximum expelled-oil yield given in bold print.
[a] X = immiscible oil yield/324.3.

In accordance with Lewan and Ruble (2002), a first-order reaction rate for generation of immiscible oil was evaluated with the time-series experiments including the 72-h runs. A first-order rate constant (k_T) for a given temperature (T) can be expressed as

$$k_T = (\mathrm{Ln}\{1/[1 - X_T]\})/\boldsymbol{t}, \quad (2)$$

where $\boldsymbol{t}$ is the duration of the experiment and X_T is the fraction of reaction completed at a given temperature (T). Using the maximum yields for ST-4[u] and RR-45[2], the fraction of reaction (X; transformation ratio) can be determined for each of the experimental yields as given in Tables 3 and 4. Plotting these values versus the duration for each time-series experiment results in a linear relation for each temperature considered in the time-series experiments (i.e., 320, 330, 340, and 350 °C). As shown by Eq. (2), the slope of this linear relation for each temperature is the rate constant.

Fig. 7 shows that a first-order reaction rate describes the immiscible oil generated from sample ST-4[u] in the time-series experiments. The slope of these linear expressions gives the rate constants for the temperatures used in the time-series experiments (Table 5). The intercepts at time zero represent the amount of reaction that occurred during the warm-up and cool-down periods. The decrease in intercept ($\boldsymbol{b}$) with decreasing experimental temperature (K) can be described by the empirical expression:

$$\mathrm{Ln}\ \boldsymbol{b} = -19817.32(1/K) + 31.4716. \quad (3)$$

This intercept at temperatures of 275 °C or less is insignificant ($X < 0.01$), and therefore, not critical in determining timing and extent of immiscible-oil generation under natural burial conditions in the subsurface. Using Eq. (3) to determine intercepts and Eq. (2) to determine the first-order reaction expression, rate constants for the temperature-series (72 h) experiments at 300 and 310 °C were be determined. These rate constants are given in Table 5.

Plotting the natural log of all of the rate constants versus the reciprocal of their experimental temperature ($1/K$) yields an Arrhenius plot. As shown in Fig. 8, a linear expression adequately describes the rate constants according to the Arrhenius expression (Eq. (1)) with the slope equating to an activation energy (E_a) of 42.784 kcal/mol and the intercept equating to a frequency factor (A_o) of $2.414 \times 10^{13}\ \mathrm{h}^{-1}$.

Fig. 9 shows that a first-order reaction rate describes the immiscible oil generated from sample RR-45[u] in the time-series experiments. Similar to ST-4[u], the slope of these linear expressions gives the rate constants for the temperatures used in the time-series experiments (Table 5). The intercepts at time zero represent the amount of reaction that occurred during the warm-up and cool-down periods. With the exception of the 340 °C-time series, the decrease in intercept ($\boldsymbol{b}$) with decreasing experimental temperature (K) can be described by the empirical expression:

$$\mathrm{Ln}\ \boldsymbol{b} = -13859.59(1/\mathrm{K}) + 19.7764 \quad (4)$$

These intercepts are considerably less than those for the ST-4[u] sample (Eq. (3)). Intercepts at temperatures of 295 °C or less are insignificant ($X < 0.01$), and therefore, not critical in determining timing and extent of immiscible oil generation under natural burial conditions in the subsurface. Using Eq. (4) to determine intercepts and Eq. (2) to determine the first-order reaction expression, rate constants for the temperature-series (72 h) experiments at 310 and 355 °C were be determined. These rate constants are given in Table 5. The negative intercept for the 340 °C-time series did not agree with Eq. (4), which gives an intercept of

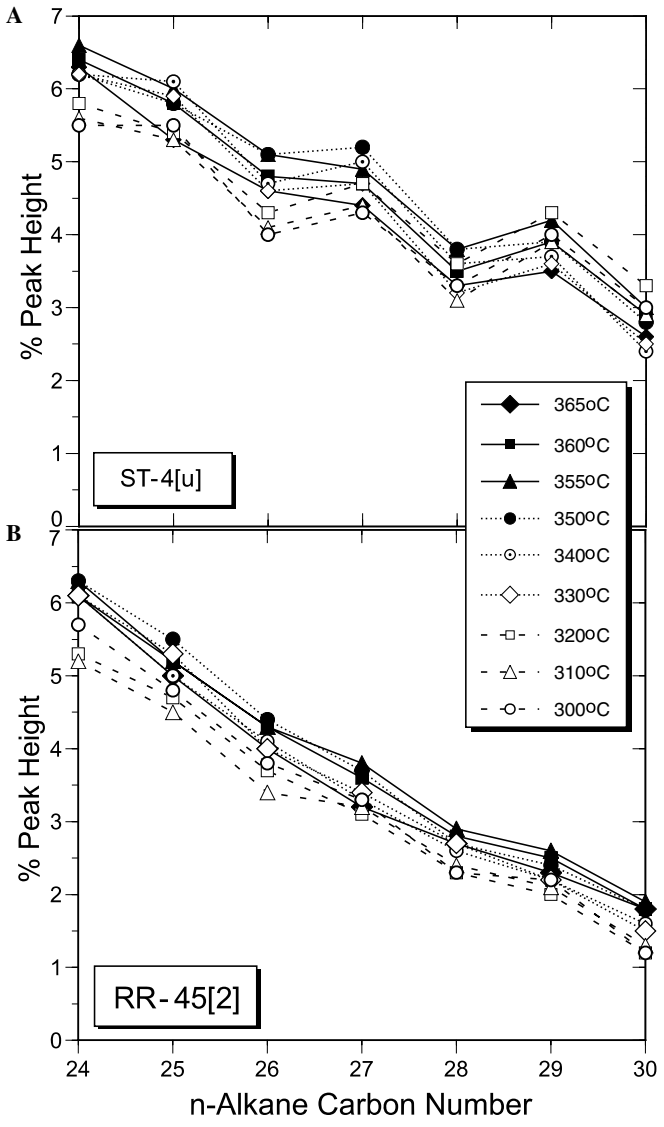

Fig. 5. Distribution of n-C_{24} to n-C_{30} alkanes based on normalized gas-chromatogram peak heights from n-C_{17} to n-C_{30} n-alkanes in immiscible oils generated by hydrous pyrolysis at 300–365 °C for 72-h durations from samples (A) ST-4[u] and (B) RR-45[2]. Immiscible oils were analyzed as whole oils in a split mode on a DB1 column of a Hewlett-Packard 6890 gas chromatograph.

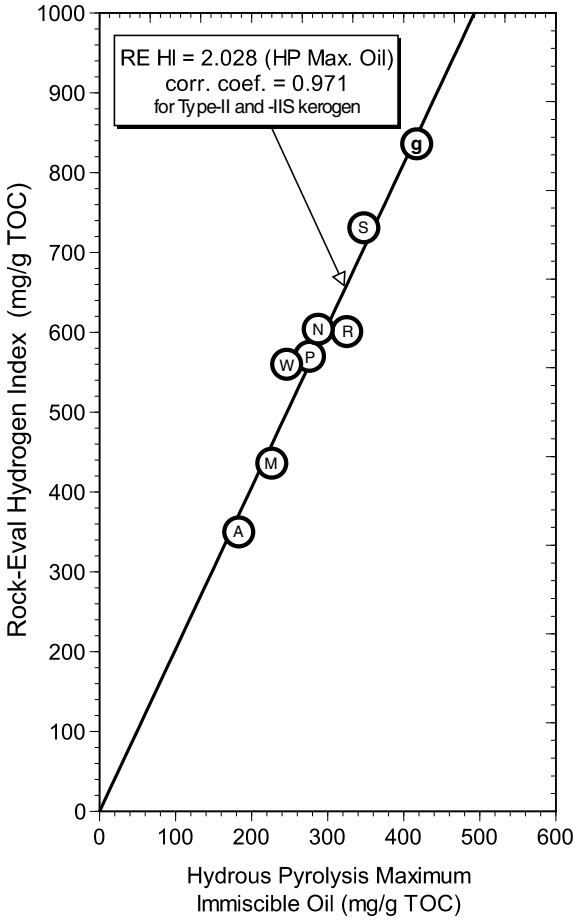

Fig. 6. Plot of maximum immiscible-oil yield from hydrous pyrolysis versus the Rock-Eval hydrogen index of the original immature sample used in the hydrous-pyrolysis experiments. Data points include samples ST-4[u] (S) and RR-45[2] (R) from this study, samples of Woodford Shale (W), New Albany Shale (N), Phosphoria Fm. (P), Monterey Fm. (M), and Alum Shale (A) from Lewan and Ruble (2002), and a sample of the Ghareb Limestone (g) from Amrani et al. (2005).

0.059. Forcing a first order expression through this calculated intercept value yields a slightly lower rate constant as shown in Table 5 and Fig. 9. However, this reduction in rate does not make a significant difference in the Arrhenius plot as shown in Fig. 10. A linear expression adequately describes the rate constants according to the Arrhenius expression (Eq. (1)), with an activation energy (E_a) of 53.946 kcal/mol and a frequency factor (A_o) of 1.814×10^{17} h^{-1}.

Fig. 11 shows that the activation energies (E_a) and frequency factors determined for samples ST-4[u] and RR-45[2] have the same compensation effect reported for Type-II, -IIS, and -I kerogen in other source rocks (Lewan and Ruble, 2002). The slope of the relationship equates to an isokinetic temperature (β) of 393 °C for immiscible oil generation. As the name implies, the rate of immiscible oil generation is the same for all kerogen types at this temperature. However, irrespective of different time-temperature conditions, the timing of oil generation from each of the kerogen types will follow the same order as long as the temperatures do not exceed 393 °C. Therefore, below this isokinetic temperature, the Monterey sample (M) will always generate oil before the Phosphoria sample (P), and the ST-4[u] sample will always generate oil before the RR-45[2] sample.

The compensation relation is attributed to a common reaction mechanism that varies in rate as a result of differences in the types or concentrations of catalysts, inhibitors, initiators, or solvents. The statistical significance of the compensation effect has been debated as reviewed by Connors (1990). However, as suggested by Lasaga (1998, p. 79), narrow compensation relations as observed in Fig. 11 indicate a common overall mechanism. Organic sulfur content of a immature kerogen appears to be a major cause of this relation. Lewan

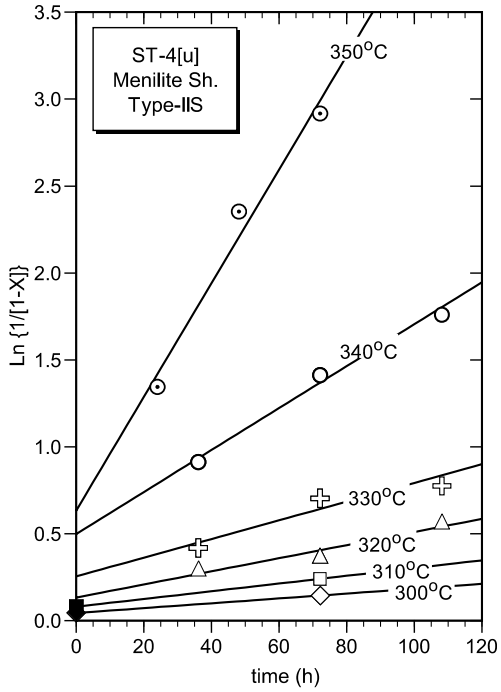

Fig. 7. Plot of first-order rate function versus time at designated temperatures for sample ST-4[u] (Type-IIS kerogen).

Table 5
First-order rate constants (k), zero-time intercepts, and correlation coefficients for immiscible oil generation from samples ST-4[u] and RR-45[2]

Temperature (°C)	k ($\times 10^{-3}$ h^{-1})	Zero-time (Ln{1/[1 − X]})	Correlation coefficient
ST-4[u]			
350	32.696	0.6334	0.987
340	12.062	0.4991	0.994
330	5.377	0.2550	0.943
320	3.771	0.1331	0.952
310[a]	2.224	0.0804	NA
300[a]	1.395	0.0444	NA
RR-45[2]			
355[a]	36.558	0.1019	NA
350	19.994	0.0844	NA
340	10.659	−0.0308	1.000
340[b]	9.593	0.0588	0.995
330	4.637	0.0406	1.000
320	2.219	0.0274	0.981
310[a]	1.239	0.0184	NA

NA = not applicable.
[a] Based on 72 h experiment and calculated intercept.
[b] Corrected for calculated zero-time intercept of 0.0588.

(1998) has shown that increasing the concentration of sulfur-radical initiators enhances the rate of free-radical reactions, and this enhancement can explain the negative correlation between activation energies for immiscible-oil generation and the kerogen organic-sulfur content. The relation between activation energies (E_a) and kerogen organic-sulfur mole fraction ($S_{org}/[S_{org} + C]$) of the ST-4[u] and RR-45[2] samples agrees with the previously reported relation by Lewan and Ruble (2002) as shown

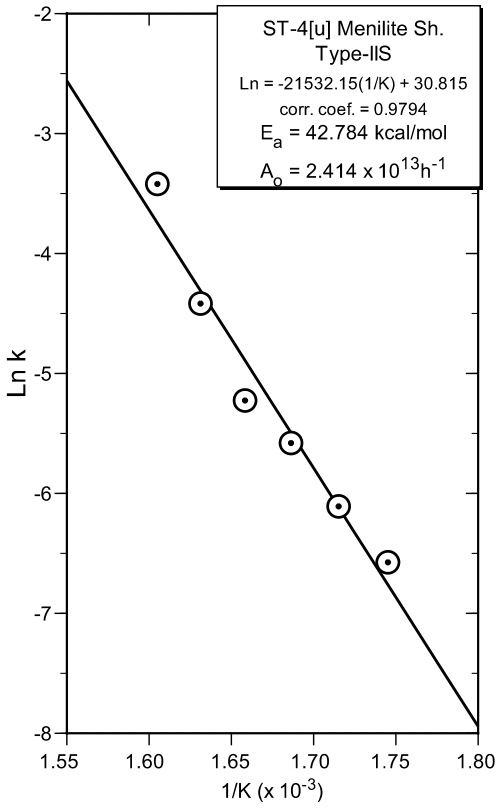

Fig. 8. Arrhenius plot of rate constants versus the reciprocal of temperature for sample ST-4[u].

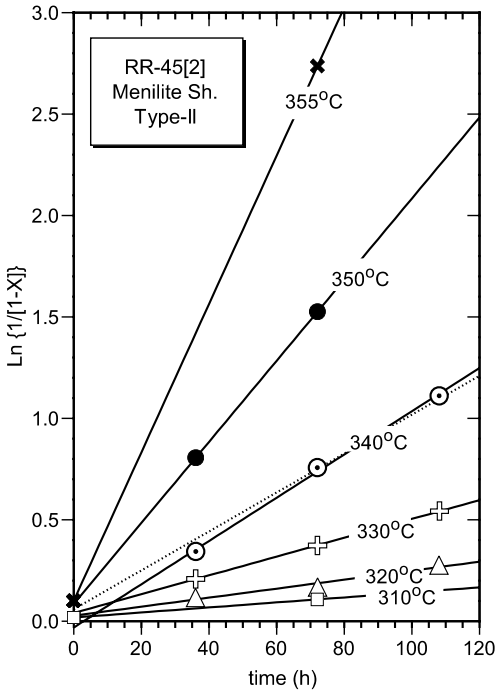

Fig. 9. Plot of first-order rate function versus time at designated temperatures for sample RR-45[2] (Type-II kerogen).

in Fig. 12. This relation allows for indirect determination of hydrous-pyrolysis activation energies of source rocks with Type-II, -IIS, and -I kerogen on the basis

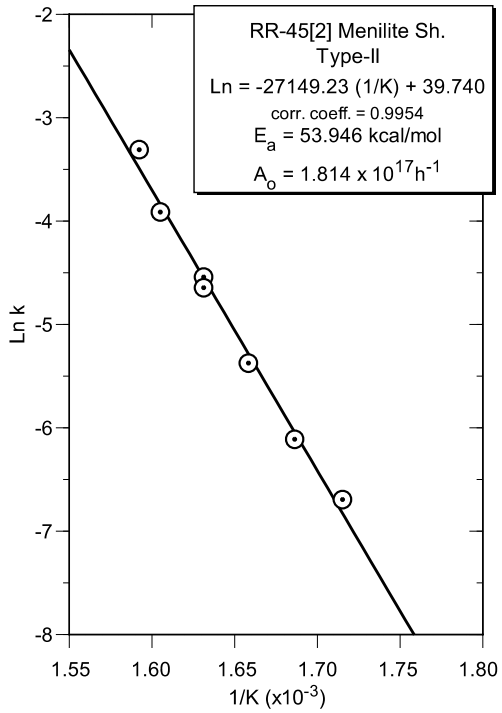

Fig. 10. Arrhenius plot of rate constants versus the reciprocal of temperature for sample RR-45[2]. Regression line includes both 340 °C-rate constants given in Table 5.

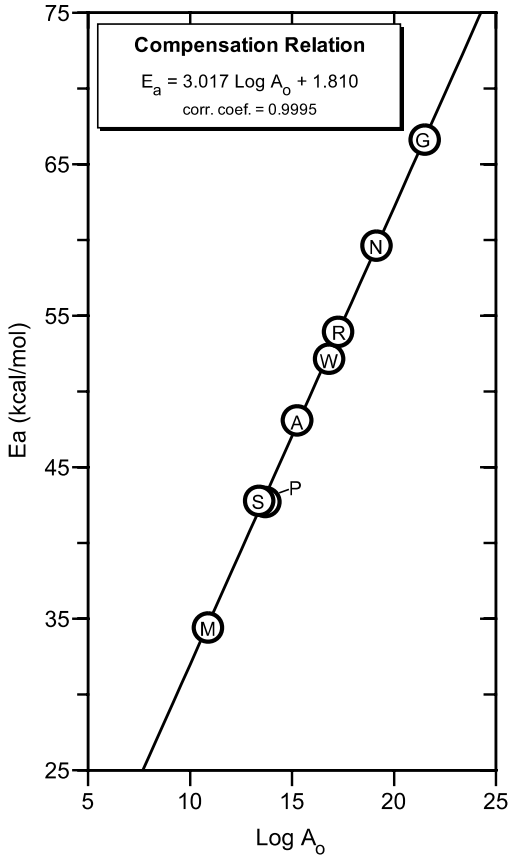

Fig. 11. Plot of compensation relation between activation energies (E_a) and log of frequency factors (A_o in 1/h) derived by hydrous pyrolysis for samples ST-4[u] (S) and RR-45[2] (R) from this study, and samples of Green River Fm. (G), Woodford Shale (W), New Albany Shale (N), Phosphoria Fm. (P), Monterey Fm. (M), and Alum Shale (A) from Lewan and Ruble (2002).

of their organic-sulfur content ($S_{org}/[S_{org} + C]$). The appropriate frequency factor can then be indirectly determined from the compensation relation (Fig. 11). This indirect determination of hydrous-pyrolysis kinetic parameters may prove particularly useful when sufficient time or sample is not available for complete experimental determinations.

3.2. Open-system pyrolysis

The discrete activation energies and frequency factors for samples ST-4[u] and RR-45[2] are given in Table 6. The frequency factors are similar for the two samples but their activation-energy distributions are different. The activation-energy distribution for sample ST-4[u] is broad with activation energies ranging from 42 to 59 kcal/mol. Sample RR-45[2] has a narrower activation-energy distribution ranging from 52 to 57 kcal/mol. More than 87 percent of S_2 generation from sample RR-45[2] is determined by one activation energy of 52 kcal/mol. Conversely, 90 percent of S_2 generation from ST-4[u] requires activation energies from 48 to 55 kcal/mol. Irrespective of these differences, S_2-generation curves calculated from the E_a distributions replicate the measured S_2-generation curves for all five heating rates (Fig. 13).

Fig. 14 shows the frequency factors and weighted-mean activation energies for both samples plot near the compensation relation for the hydrous-pyrolysis kinetic parameters (Fig. 12). However, the open-system kinetic parameters plot closer to one another than the hydrous-pyrolysis kinetic parameters. As a result, kinetic parameters determined by open-system pyrolysis show less difference in mean S_2-generation rates than oil-generation rates determined by hydrous-pyrolysis kinetic parameters. This result is in agreement with the comparative study of other source rocks by Lewan and Ruble (2002).

3.3. Burial histories

Before extrapolating these kinetic parameters into the structurally complex burial history of the Paszowa-1 well, a simple hypothetical burial history will provide a more lucid comparison of these different kinetic parameters and their geological implications. Temperature and time are the two critical geological inputs considered in the Arrhenius equation (Eq. (1)). They can be treated collectively as a heating rate (°C/m.y.), which typically ranges from 1 to 10 °C/m.y. in sedimentary basins (Gretener and Curtis, 1982). Using these two geological heating rates, hypothetical burial histories were constructed using the kinetic parameters derived from open-system and hydrous pyrolysis. As shown in Fig. 15, generation curves span a broad time interval (37–101 m.y.) at the slower heating rate and

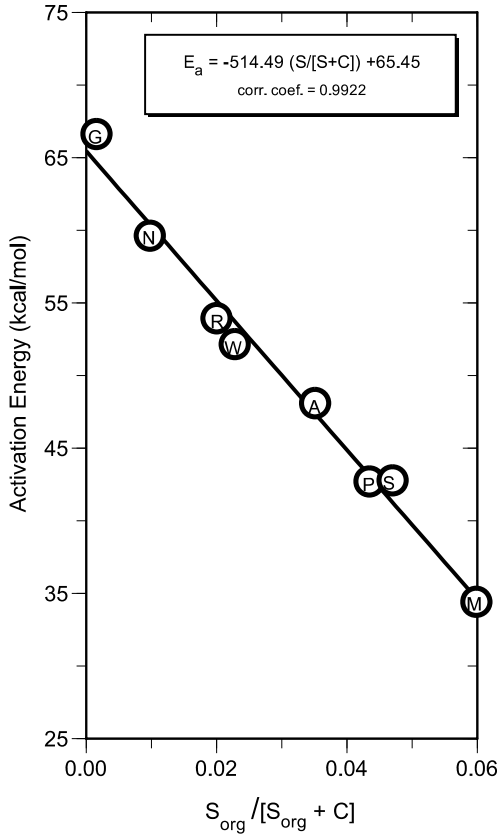

Fig. 12. Relation between organic-sulfur mole fraction ($S_{org}/[S_{org} + C]$) of immature kerogen and activation energy derived from hydrous pyrolysis for generation of immiscible oil from samples ST-4[u] (S) and RR-45[2] (R) of this study, and from samples of Green River Fm. (G), Woodford Shale (W), New Albany Shale (N), Phosphoria Fm. (P), Monterey Fm. (M), and Alum Shale (A) of Lewan and Ruble (2002).

Table 6
Open-system kinetic parameters determined for first-order reactions with a discrete activation-energy distributions for samples ST-4[u] and RR-45[2]

Discrete E_a (kcal/mol)	ST-4[u] (x_i)	RR-45[2] (x_i)
42	0.0008	0.0
43	0.0013	0.0
44	0.0066	0.0
45	0.0	0.0
46	0.0101	0.0
47	0.0253	0.0
48	0.0610	0.0
49	0.0703	0.0
50	0.1273	0.0
51	0.0993	0.0
52	0.1965	0.8786
53	0.1463	0.0
54	0.1407	0.1144
55	0.0612	0.0
56	0.0249	0.0
57	0.0158	0.0070
58	0.0	0.0
59	0.0126	0.0
Weighted-mean E_a (kcal/mol)	51.8	52.3
Frequency factor A_o (h^{-1})	2.57×10^{17}	8.496×10^{16}

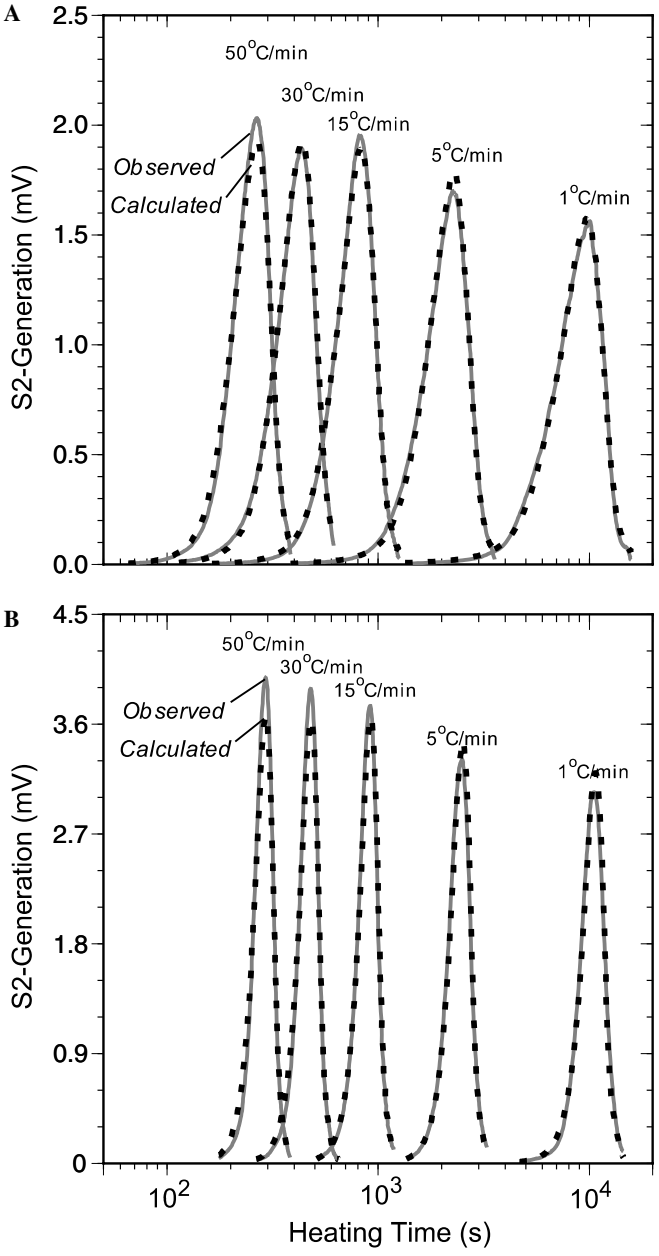

Fig. 13. Plot showing the observed (solid line) and calculated (dashed line) S_2 generation at five heating rates for (A) sample ST-4[u] and (B) sample RR-45[2]. The observed curves are from the SR analyzer (open-system pyrolysis) and the calculated curves are derived from the discrete activation-energy distributions and single frequency factors given in Table 6.

a narrow time interval (4–10.5 m.y.) at the faster heating rate.

Although the time span is significantly reduced at the fast heating rate, the generation curves for the different kinetic parameters maintain their same relative position among one another. Using the transformation ratio (TR) of 0.50 (i.e., 50% generation) as a reference point, hydrous-pyrolysis kinetics for Type-IIS and -II kerogen (i.e., samples ST-4[u] and RR-45[2], respectively) determine the earliest and latest times for oil generation, respectively. The open-system pyrolysis kinetic parameters occur be-

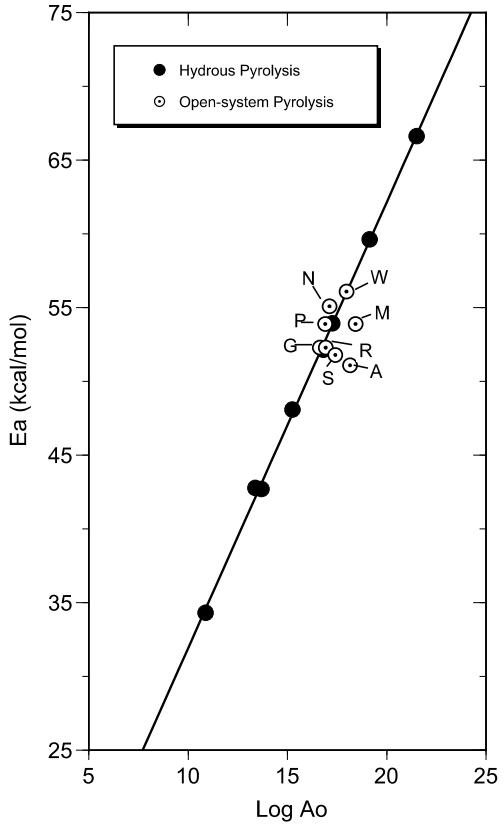

Fig. 14. Plot of mean-weighted activation energies (E_a in kcal/mol) and log of single frequency factors (A_o in 1/h) derived from open-system pyrolysis (open centered points) of samples ST-4[u] (S) and RR-45[2] (R) from this study, and samples of Green River Fm. (G), Woodford Shale (W), New Albany Shale (N), Phosphoria Fm. (P), Monterey Fm. (M), and Alum Shale (A) from Lewan and Ruble (2002). Solid points and line are compensation relation for kinetic parameters derived from hydrous pyrolysis as shown in Fig. 11.

tween the curves derived from the hydrous-pyrolysis kinetic parameters, with the Type-IIS curve occurring earlier than the Type-II curve (Fig. 15). At both heating rates, the hydrous-pyrolysis curves remain essentially parallel to one another. Conversely, the open-system pyrolysis curves converge at a transformation ratio (TR) of about 0.8, with Type-II kerogen generating sooner than Type-IIS kerogen at higher transformation ratios (Fig. 15). Another difference is the time span determined for generation. At 1 °C/m.y., the open-system pyrolysis kinetic parameters for Type-IIS and -II kerogen generate (TR = 0.01–0.99) over time spans of 101 and 51 m.y., respectively. The hydrous-pyrolysis kinetic parameters for Type-IIS and -II kerogen generate over a narrower time span of 39 and 37 m.y., respectively. At 10 °C/m.y., the open-system pyrolysis kinetic parameter for Type-IIS and -II kerogen generate (TR = 0.01–0.99) over time spans of 10.5 and 5.5 m.y., respectively. The hydrous-pyrolysis kinetic parameters for Type-IIS and -II kerogen again generate over a narrower time span of 4.5 and 4 m.y., respectively.

The average heating rate for the base of the Menilite Shales in the Paszowa-1 well prior to uplift and erosion event B is ~10 °C/m.y. Based on the hypothetical burial

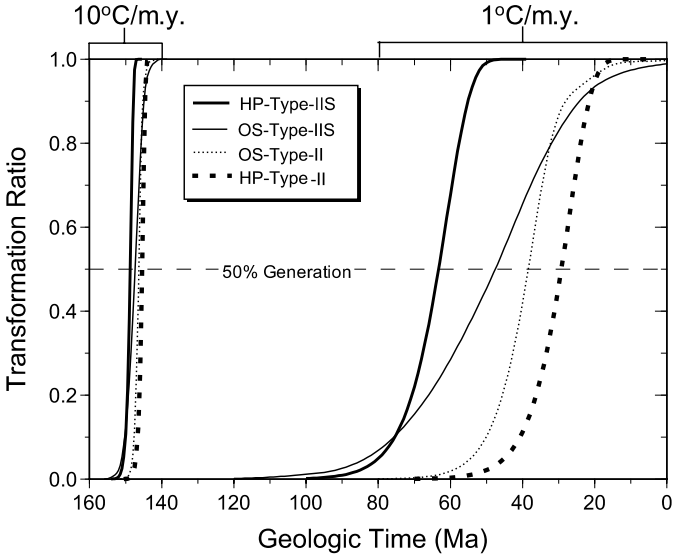

Fig. 15. Generation curves for immiscible oil generation from hydrous-pyrolysis (HP) kinetic parameters and S_2 generation from open-system pyrolysis (OS) kinetic parameters for samples ST-4[u] (Type-IIS kerogen) and RR-45[2] (Type-II kerogen) at natural heating rates of 10 and 1 °C/m.y. Surface temperature for both heating rates is 15 °C.

histories in Fig. 15, the differences in timing of generation among the open-system and hydrous-pyrolysis kinetic parameters for Type-IIS and -II kerogen will be small. This is confirmed in the burial history for the Paszowa-1 well (Fig. 16), which shows open-system and hydrous-pyrolysis kinetic parameters for both kerogen types generate within a 1.4-m.y. interval at 50% generation (TR = 0.5). This maximum spread is defined by the hydrous-pyrolysis kinetic parameters for Type-IIS kerogen at 17.2 Ma and Type-II kerogen at 15.8 Ma. Open-system pyrolysis kinetic param-

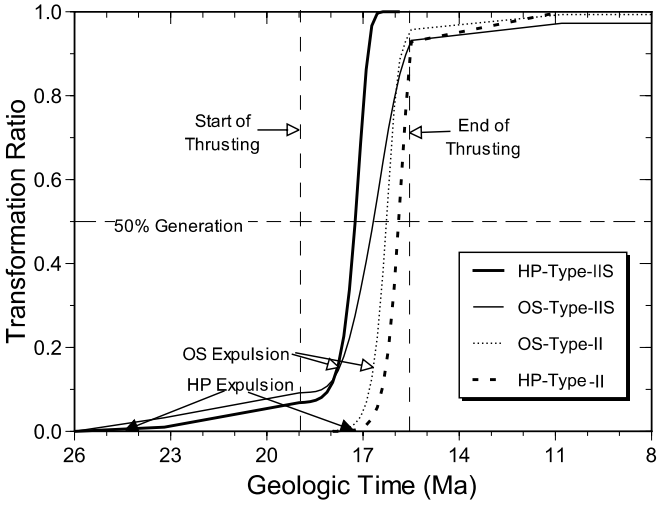

Fig. 16. Generation curves for immiscible oil generation from hydrous-pyrolysis (HP) kinetic parameters and S_2 generation from open-system pyrolysis (OS) kinetic parameters for samples ST-4[u] (Type-IIS kerogen) and RR-45[2] (Type-II kerogen) at the base of the Menilite Shales in the Paszowa-1 well as described in Table 2.

eters generate over a narrower range of 0.45 m.y. within the 1.4-m.y. interval determined by the hydrous-pyrolysis kinetic parameters at a TR of 0.5 (Fig. 16).

Although differences between generation curves determined by open-system and hydrous-pyrolysis kinetic parameters for Type-IIS and -II kerogen are small at high heating rates, their determined times of generation influences interpretations of petroleum occurrences in a structurally complex area like the Polish Carpathians. Fig. 16 shows that all of the kinetic parameters generate within the major folding and thrusting event (19–15.5 Ma), but only hydrous-pyrolysis kinetic parameters for Type-IIS kerogen predict complete generation during this time (TR = 0.99 at 16.6 Ma). The other kinetic parameters reach TRs between 0.9 and 0.95 by the end of the event (15.5 Ma). Early and complete generation of the Type-IIS kerogen as predicted by the hydrous-pyrolysis kinetic parameters could result in a greater loss of its high-sulfur oils because of the absence of early-formed traps, tectonic breaching of early traps, or erosion of traps higher in the thrust sheets. Conversely, late generation of the Type-II kerogen as predicted by the hydrous-pyrolysis kinetic parameters could result in less loss of its low-sulfur oil because of diminishing tectonic activity resulting in more stable traps that are less vulnerable to being breached. This interpretation is in general agreement with only low-sulfur oil accumulations (Curtis et al., 2004) occurring predominantly in interbedded sandstone of the Menilite Shales in folds and stratigraphic traps near the southwestern border of the Skole thrust unit (Karnkowski, 1999). Admittedly, this timing of events is intricate, but it and other renditions become untenable using the narrower times determined by the open-system pyrolysis kinetic parameters. As shown in Fig. 16, the small 0.45-m.y. difference in generation between Type-IIS and -II kerogen at a TR of 0.5 diminishes to nothing by a TR of 0.8 and then reverses order at higher TR values. This narrower time difference between generation from Type-IIS and -II kerogen would suggest that both high- and low-sulfur oils would exist in the Skole unit, which is not observed.

Start of generation for Type-IIS kerogen in the Paszowa-1 well occurs during the sedimentation of the Krosno and transitional beds as determined by the open-system and hydrous-pyrolysis kinetic parameters. However, it is important to distinguish between the products being considered by these kinetic parameters when interpreting the geological implications. Open-system pyrolysis kinetic parameters predict generation of S_2, which is rich in polars and more like bitumen than oil (Fig. 4). Therefore, timing of generation and expulsion are not the same for open-system kinetics parameters. Pepper and Corvi (1995) suggest that expulsion of oil from high-quality source rocks occurs at transformation ratios of 0.15–0.20. Other models suggest expulsion occurs at higher transformation ratios at or in excess of 0.30 (Braun and Burnham, 1991). Using the lowest prescribed TR of 0.15 for the expulsion of generated oil in predicted S_2 generation curves by open-system pyrolysis kinetic parameters, indicates that no oil from Type-IIS kerogen would be expelled prior to the major folding and thrusting in the Paszowa-1 well (Fig. 16). This makes it difficult to explain the high-sulfur oil accumulations in the Carpathian Foredeep. These oils are derived in part from the Menilite Shales and require generation and expulsion prior to major folding and thrusting (Lafargue et al., 1994).

Conversely, generation curves based on hydrous-pyrolysis kinetic parameters are based on generation of expelled immiscible oil. As observed in hydrous pyrolysis experiments (Lewan, 1987) and advocated in natural maturation (Momper, 1978), oil expulsion is a direct consequence of oil generation. This coupling of generation and expulsion is attributed to the net volume increase in generated oil, which exceeds available porosity in an already bitumen-impregnated rock (Lewan, 1987). This applies to high-quality source rocks with organic carbon contents typically in excess of 2.5 wt% (Lewan, 1987), which would be the case for source rocks in the Menilite Shales that have a mean organic carbon content of 6.7 ± 2.9 wt% (Curtis et al., 2004). As a result, hydrous-pyrolysis kinetic parameters for Type-IIS kerogen determine generation of expelled high-sulfur oil prior to the major folding and thrusting in the Paszowa-1 well (Fig. 16). This early generation and expulsion from the Type-IIS facies of the Menilite Shales makes it feasible for high-sulfur oils to migrate into the Carpathian Foredeep traps prior to folding and thrusting as suggested by Lafargue et al. (1994).

4. Discussion

4.1. Openness

One of the reasons for the lack of significant differences in timing of oil generation from Type-II and Type-IIS kerogen by open-system pyrolysis kinetic parameters has been attributed to premature removal of early-formed sulfur radicals before they initiate cracking reactions involving bitumen decomposition to oil (Lewan, 1998). Conversely, early-formed sulfur radicals are confined in the bitumen-impregnated rock during hydrous pyrolysis and their influence is reflected in the kinetic parameters for oil generation. This brings up the issue of whether natural maturation is better represented by open- or closed-system pyrolysis (e.g., Schenk et al., 1997). There is little doubt that generated oil and gas are expelled and migrate away from their source rock during natural maturation. It is this separation of expelled products that makes it difficult to correlate oil and gas accumulations with their source rocks. However, vaporization of generated polar-rich products at high temperatures (250–650 °C) and low pressures (~100–200 kPa) in open-system pyrolysis is not likely to occur in natural maturation.

The openness of natural maturation is also significantly less than open-system pyrolysis in that heating rates are more than 10 orders of magnitude slower (i.e., 10^{-12}–10^{-11} °C/min; Gretener and Curtis, 1982) and petroleum

migration rates are more than 7 orders of magnitude slower (i.e., 10^{-12}–10^{-9} m/s; England et al., 1991). At these extremely slow heating and migration rates, natural maturation has more semblances to closed-system pyrolysis than open-system pyrolysis. In hydrous pyrolysis, generated oil and gas are expelled from the source rock and, respectively, accumulate on the liquid-water surface and in the headspace of the reactor for the duration of the experiments (Lewan, 1993). These expelled products are separated from the source rock by liquid water throughout the duration of the experiment. The foremost closed aspect of hydrous pyrolysis is that the expelled products remain in the same temperature and pressure regime as their maturing source rock. As shown in Figs. 3–5, the thermal and pressure regime in experiments at 300–365 °C for 72-h durations does not significantly alter the immiscible oil. Although hydrous pyrolysis is a closed system, it may be more representative of the degree of openness in natural maturation than that of open-system pyrolysis.

4.2. Products

The S_2 product measured by open-system pyrolysis does not differentiate between initial kerogen decomposition to polar-rich bitumen and subsequent bitumen decomposition to hydrocarbon-rich oil. The high polar content of the S_2 product (Fig. 4) indicates that a significant amount of the bitumen generated from the initial decomposition of kerogen is volatilized and removed from the open-system before it can decompose into hydrocarbon-rich oil. As a result, the kinetic parameters from open-system pyrolysis are highly influenced by kerogen decomposition to bitumen with inclusion of some undetermined portion of bitumen decomposition to oil. This bitumen-rich S_2 product may minimize differences in the timing of oil generation that result in a narrower range of weighted-mean activation energies (51.8–52.3 kcal/mol, Table 6) and frequency factors (8.496×10^{16} and 2.57×10^{17} h^{-1}, Table 6), and the lack of, a compensation relation (Fig. 14). This is in contrast to the kinetic parameters based on generation of immiscible oil in hydrous pyrolysis. These kinetic parameters show a wider range of activation energies (42.8–53.9 kcal/mole) that equate to organic-sulfur contents (Fig. 12) and their frequency factors (Fig. 11).

The skewed distribution of activation energies toward lower values for Type-IIS kerogen determined by open-system pyrolysis (Table 6) does result in earlier S_2 generation than the less skewed distribution of the Type-II kerogen. However, this earlier S_2 generation is more likely representative of earlier generation of bitumen from kerogen than oil from bitumen. At transformation ratios above about 0.1, the parallelism between the S_2-generation curves for Type-IIS and -II kerogen ceases and the early generation of Type-IIS kerogen begins to lessen and converges on the generation curve of the Type-II kerogen (Figs. 15 and 16). The generation curve of the Type-IIS kerogen merges with that of the Type-II kerogen at a transformation ratio of about 0.8. At higher transformation ratios, the two curves become sub-parallel to one another with only a small difference (Figs. 15 and 16). This convergence is interpreted as the kinetics for bitumen to oil generation for Type-IIS and -II kerogen being essentially the same in open-system pyrolysis, with the earlier S_2 generation from Type-IIS kerogen being a result of earlier generation of bitumen from the sulfur-enriched kerogen. Although this interpretation is consistent with kinetic data for the samples with Type-IIS and Type-II kerogen in this study, other kinetic studies using open-system pyrolysis do not always show the influence of early bitumen generation from Type-IIS kerogen (Reynolds et al., 1995; Lewan and Ruble, 2002).

4.3. Temperature

Another consideration is the temperature at which the kinetic parameters are determined in open-system and hydrous pyrolysis. As temperature increases the selectivity of initiating radicals can diminish significantly (March, 1985, p. 613). Hass et al. (1936) showed that a chlorine radical is 7 times more likely to abstract a tertiary hydrogen and 4.3 times more likely to abstract a secondary hydrogen than a primary hydrogen from an alkane at 100 °C. This selectivity at 600 °C is significantly reduced with same chlorine radical being only 2.6 times more likely to abstract a tertiary hydrogen and 2.1 times more likely to abstract a secondary hydrogen than a primary hydrogen. As a result, critical rate-controlling reaction mechanisms operating at the lower temperatures used in hydrous pyrolysis and natural maturation may not be as discriminating or influential at the higher temperatures used in open-system pyrolysis. As a result, the kinetic parameters derived from hydrous pyrolysis would be more controlled by the selectivity of initiating radicals and nuances in the molecular structure of a bitumen.

In addition to less selectivity at higher temperatures, the compensation relation (Fig. 11) indicates that reaction rates will converge on the same reaction rate at an isokinetic temperature, which is 393 °C for the hydrous-pyrolysis kinetic parameters. This relation is shown in Fig. 17 for the kerogen types used in this study and those reported by Lewan and Ruble (2002). Reaction rates increase and diverge at temperatures above this isokinetic temperature and decrease and diverge at temperatures below this isokinetic temperature. Interestingly, the succession of kerogen types with respect to their reaction rates reverses at temperatures greater than the isokinetic temperature. Faster reacting Type-IIS kerogen below the isokinetic temperature becomes the slower reacting kerogen above the isokinetic temperature. This theoretical reversal has not been verified by experiments. However, the critical aspects of this relation is that as experimental temperatures approach or include the isokinetic temperature, the reaction rates for the different kerogen types become less distinguishable.

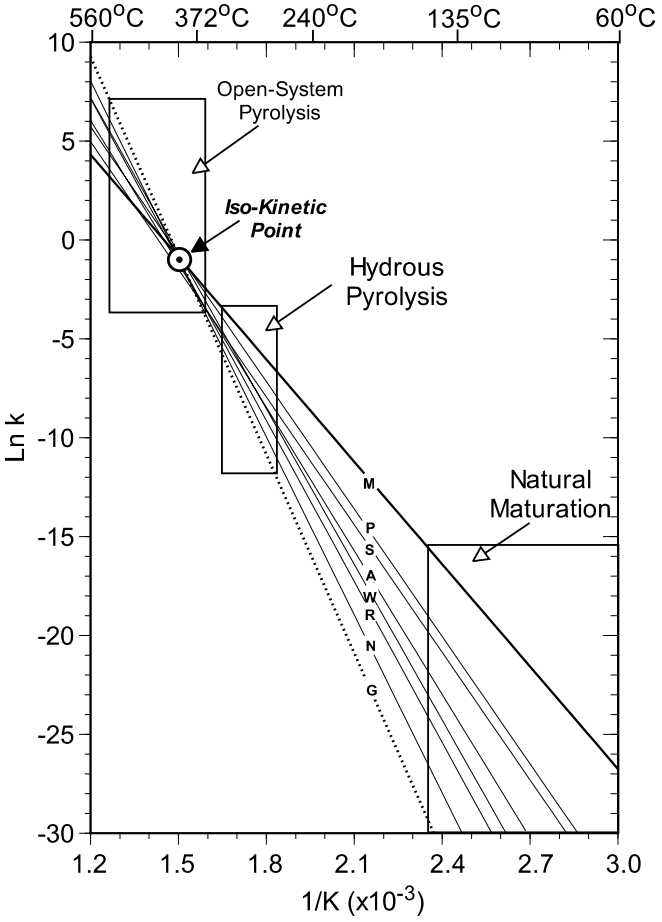

Fig. 17. Arrhenius plot showing the extended relations of hydrous-pyrolysis kinetic parameters to higher and lower temperatures. The isokinetic temperature (393 °C) as determined by the compensation relation (Fig. 11) is denoted along with thermal regimes for open-system and hydrous pyrolysis between TRs of 0.1 and 0.9. Thermal regime for natural maturation is based on a temperature of 150 °C. Symbols for the different Arrhenius relations are the same as in Fig. 14.

Superimposed on Fig. 17 are the temperature ranges representing transformation ratios from 0.1 to 0.9 for open-system and hydrous pyrolysis and the approximate temperature range for natural maturation. The broad range of reaction rates at temperatures below 150 °C indicates that the extrapolated kinetic parameters from hydrous pyrolysis have a significant influence on determining the timing of oil generation during natural maturation. This significance in natural maturation has been shown to be particularly important for Type-IIS kerogen (Lewan, 2002; Lewan and Ruble, 2002) and for low-sulfur Type-I kerogen (Ruble et al., 2001). The temperature range used to determine rate constants by hydrous pyrolysis appears to be the most optimum. They represent the lowest possible temperatures to obtain rate constants within practical laboratory times, and they are sufficiently below the isokinetic temperature to realize measurable differences between the kerogen types. Assuming some portion of S_2 generation represents the conversion of bitumen to oil observed in hydrous pyrolysis, the temperature range used to determine rate constants by open-system pyrolysis is less optimum. As shown in Fig. 17, this higher temperature range includes the isokinetic temperature and the narrow range of rate constants on both sides of it. The significance of this difference is observed by comparing the mean differences in rate constants between the two extreme kerogen types (i.e., Green River Type-I (G) and Monterey Type-IIS (M)). Despite the broader temperature range of the open-system pyrolysis, the mean difference in rate constant is only 3.4 h^{-1} compared with 25.6 h^{-1} for hydrous pyrolysis over a narrower temperature range.

4.4. Concurrence

Although diminished reaction selectivity and reaction-rate differences at the higher temperatures used in open-system pyrolysis results in less discriminating kinetic parameters, these kinetic parameters appear to give comparable timings of oil generation for typical marine source rocks with Type-II kerogen. This similarity is shown in the hypothetical (Fig. 15) and Paszowa-1 (Fig. 16) burial histories. The average mean-weighted activation energy of the distributions for the two samples in this study and the six reported by Lewan and Ruble (2002) is 53.31 ± 1.73 kcal/ mol with an average frequency factor of 2.78×10^{17} h^{-1}. These average values are similar to the kinetic parameters from hydrous pyrolysis of Type-II kerogen with $S_{org}/[S_{org} + C]$ mole fractions between of 0.02 and 0.03 (i.e., RR-45[2] and Woodford Shale). This is within the range of typical Type-II kerogen of marine clastic source rocks (i.e., 0.016–0.030, Orr and Sinninghe-Damsté, 1990). Therefore, kinetic parameters determined by open-system and hydrous pyrolysis for Type-II kerogen within this range of $S_{org}/[S_{org} + C]$ mole fractions give similar times of oil generation in natural maturation. It is only when the $S_{org}/[S_{org} + C]$ mole fractions are greater or less than this range that deviations in kinetic parameters result in significant differences for the timing of oil generation during natural maturation.

5. Conclusions

The Menilite Shales of the Polish Carpathians have provided an opportunity to compare timing and extent of petroleum generation from two different organic facies (Type-II and -IIS kerogen) in a natural high-heating rate regime with kinetic parameters determined by open-system and hydrous pyrolysis. As expected, the high heating rates minimize the timing differences between the Type-IIS and -II kerogen types, but the differences determined by kinetic parameters derived from hydrous pyrolysis have significant geologic implications. The most significant difference is the early generation of expelled oil from Type-IIS kerogen prior to major thrusting as determined by hydrous-pyrolysis kinetic parameters. This timing explains the high-sulfur oils found in the Carpathian

Foredeep that have been correlated to the Menilite Shales. Kinetic parameters derived from open-system pyrolysis indicate some S_2 generation would have occurred prior to major thrusting, but the expulsion of oil would not occur until after the start of major thrusting.

At transformation ratios greater than 0.5, kinetic parameters derived from open-system pyrolysis show no significant differences in S_2 generation for Type-IIS and -II kerogen types. Conversely, kinetic parameters derived from hydrous pyrolysis show significant and consistent differences in immiscible oil generation from transformation ratios of 0.01–0.99. This difference is similar to those previously published (Lewan and Ruble, 2002), which suggest that the effects of sulfur-radical initiators responsible for oil generation are not fully realized in open-system pyrolysis. The lack of significant differences in timing shown by open-system kinetic parameters for Type-IIS and -II kerogen may also be attributed to bitumen being a prominent component of the S_2 product, and to reduced radical selectivity and divergence of reaction rates at the higher operating temperatures.

Results of this study support previously published relations that can be used to indirectly determine hydrous-pyrolysis kinetic parameters. The kinetic parameters for the Type-IIS and -II kerogen samples used in this study support the correlation between the $S_{org}/[S_{org} + C]$ mole fraction of kerogen and its activation energy (Lewan, 1998; Lewan and Ruble, 2002). This relation allows for the indirect determination of activation energies by determining the organic sulfur and carbon contents of immature Type-IIS and -II kerogen. The compensation effect previously reported for kinetic parameters determined by hydrous pyrolysis (Lewan and Ruble, 2002) is also supported by the two samples used in this study. With this relation, the frequency factor can be determined from the activation energy determined from the organic-sulfur mole fraction. Therefore, when limited time or sample precludes determining kinetic parameters by hydrous pyrolysis, hydrous-pyrolysis kinetic parameters can be determined indirectly by determining the $S_{org}/[S_{org} + C]$ mole fraction of immature kerogen.

This study also established a reliable correlation between the maximum yield of immiscible oil generated by hydrous pyrolysis and the hydrogen index (HI; S_2/organic carbon) obtained by open-system pyrolysis. Determining the maximum yield of immiscible oil generated is a required value in deriving kinetic parameters from hydrous pyrolysis. This relation provides a means of determining this maximum value from the open-system pyrolysis of a source rock containing Type-IIS and -II kerogen. The relation indicates that the maximum amount of immiscible oil generated by hydrous pyrolysis represents only about one half of the S_2 generated by open-system pyrolysis. The other unaccounted for half of S_2 generated in open-system pyrolysis consists of polar components that represent bitumen.

Acknowledgments

This research was undertaken as part of the American-Polish geochemical research project on the Polish Carpathians funded by the Joint Maria Skłodowska-Curie II Fund (Grant MEN/USGS-97-319). The authors acknowledge and appreciate the analytical support provided by Michael Pribil, Augusta Warden, and Nicholas Battaglia (USGS). Review comments and suggestions by David King (USGS), Tim Ruble (Humble Geochemical Services), Eli Tannenbaum (Kimron Oil and Minerals), and two anonymous reviewers were helpful in the early versions of the manuscript. The authors are especially grateful for the advice of Dr. Jan Kuśmierek on the burial history and geology of the area.

Associate editor: Jeffrey Seewald

References

Amrani, A., Lewan, M.D., Aizenshtat, Z., 2005. Stable sulfur isotope partitioning during simulated petroleum formation as determined by hydrous pyrolysis of Ghareb Limestone, Israel. *Geochim. Cosmochim. Acta* **69**, 5317–5331.

Behar, F., Vandenbroucke, M., Tang, Y., Marquis, F., Espitalie, J., 1997. Thermal cracking of kerogen in open and closed systems: determination of kinetic parameters and stoichiometric coefficients for oil and gas generation. *Org. Geochem.* **26**, 321–339.

Bessereau, G., Roure, F., Kotarba, M., Kuśmierek, J. Strzetelski, W. (1996). Structure and hydrocarbon habitat of the Polish Carpathians. In: Ziegler, P.A., Horvath, F. (Eds.), *Structure and Prospects Alpine Basins and Forelands*. Peri-Tethys Memoir 2, Mémoires du Museum National d'Histoire Naturelle 170, Paris, pp. 343–373.

Braun, R.L., Burnham, A.K., 1991. PMOD: a flexible model of oil and gas generation, cracking, and expulsion. *Org. Geochem.* **19**, 161–172.

Braun, R.L., Rothman, A.J., 1975. Oil-shale pyrolysis: kinetics and mechanisms of oil production. *Fuel* **54**, 129–131.

Burnham, A.K., Braun, R.L., 1999. Global kinetic analysis of complex materials. *Energy Fuels* **13**, 1–22.

Butler, E.B., Barker, C., 1986. Kinetics of bitumen release from heated shale. *Geochim. Cosmochim. Acta* **50**, 2281–2288.

Cieszkowski, M., Ślączka, A., Wdowiarz, S., 1985. New data on structure of the Flysch Carpathians. *Przegl. Geol.* **33**, 313–328.

Connors, K.A., 1990. *Chemical Kinetics: The Study of Reaction Rates in Solution*. VCH, New York, 480 p.

Curtis, J.B., Kotarba, M.J., Lewan, M.D., Więcław, D., 2004. Oil/source rock correlations in the Polish Flysch Carpathians and Mesozoic basement and organic facies of the Oligocene Menilite Shales: insights from hydrous pyrolysis experiments. *Org. Geochem.* **35**, 1573–1596.

England, W.A., MacKenzie, A.S., Mann, D.M., Quigley, T.M., 1991. The movement and entrapment of petroleum fluids in the subsurface. *J. Geol. Soc. London* **144**, 327–347.

Franks, A.J., Goodier, B.D., 1922. Preliminary study of the organic matter of Colorado oil shales. *Q. Colo. Sch. Mines* **17**, 3–16.

Gretener, P.E., Curtis, C.D., 1982. Role of temperature and time on organic metamorphism. *Am. Assoc. Petrol. Geologists Bull.* **66**, 1124–1129.

Hass, H.B., McBee, E.T., Weber, P., 1936. Chlorination of paraffins: factors affecting yields of isomeric monochlorides and dichlorides. *Ind. Eng. Chem.* **28**, 333–339.

ten Haven, H.L., Lafargue, E., Kotarba, M., 1993. Oil/oil and oil/source rock correlations in the Carpathian Foredeep and Overthrust, southeast Poland. *Org. Geochem.* **20**, 935–959.

Huizinga, B.J., Aizenshtat, Z.a., Peters, K.E., 1988. Programmed pyrolysis-gas chromatography of artificially matured Green River kerogen. *Energy Fuels* **2**, 74–81.

Jarvie, D.M., Weldon, W.D., Leroux, B., Walker, P.R. (1996). Automated Thermal Extraction and Pyrolysis Total Petroleum Hydrocarbon and Kinetic Analysis using the SR Analyzer. Pittsburgh Conference on Analytical Chemistry and Spectroscopy Abstracts, Chicago, Illinois, Paper 785.

Karnkowski, P., 1999. *Oil and Gas Deposits in Poland* [W. Górecki, Trans.]. Geosynoptics Society, University of Mining and Metallurgy, Kraków, 380 p.

Kotlarczyk, J., Leśniak, T., 1990. *Lower part of the Menilite Formation and related Futoma Diatomite Member in the Skole Unit in the Polish Carpathians*. Wydawnictwo Akademii Górniczo-Hutniczej, Kraków, 74 p.

Kruczek, J., 1999. Recent tectonic surveys of the Carpathian Flysch in Krosno-Sanok-Gorlice area. *Prace Instytut Górnictwa Naftowego i Gazownictwa* **98**, 1–34.

Książkiewicz, M., 1977. The tectonics of the Carpathians. In: Pożaryski, W. (Ed.), *Geology of Poland*, *Tectonics*, vol. 4. Wydawnictwo Geologiczne, Warszawa, pp. 476–620.

Kuśmierek, J., 1996. Evolution of the central Carpathian oil basin-quantitative interpretation. In: Roure, F., Ellouz, N., Shein, V.S., Skvortsov, I.I. (Eds.), *Geodynamic Evolution of Sedimentary Basins*. Éditions Technip, Paris, pp. 281–303.

Kuśmierek, J., Maćkowski, T. (1995). Calibration of paleothermal regime. In: J. Kuśmierek (ed.). Evolution and Hydrocarnon Potential of the Polish Carpathians. Geol. Trans. Pol. Acad. Sci., No. 138, 55–63.

Lafargue, E., Ellouz, N., Roure, F., 1994. Thrust-controlled exploration plays in the outer Carpathians and their foreland (Poland, Ukraine and Romania). *First Break* **12**, 69–79.

Lasaga, A.C., 1998. *Kinetic Theory in the Earth Sciences*. Princeton University Press, Princeton, 811 p.

Lewan, M.D., 1978. Laboratory classification of very fine-grained sedimentary rocks. *Geology* **6**, 745–748.

Lewan, M.D. (1980) Geochemistry of Vanadium and Nickel in Organic Matter of Sedimentary Rocks. Ph.D. Dissertation, University of Cincinnati, 353 p.

Lewan, M.D., 1985. Evaluation of petroleum generation by hydrous pyrolysis experimentation. *Philos. Trans. R. Soc. London* **A315**, 123–134.

Lewan, M.D., 1987. Petrographic study of primary petroleum migration in the Woodford Shale and related rock units. In: Doligez, B. (Ed.), *Migration of Hydrocarbons in Sedimentary Basins*. Éditions Technip, Paris, pp. 113–130.

Lewan, M.D., 1993. Laboratory simulation of petroleum formation: hydrous pyrolysis. In: Engel, M., Macko, S. (Eds.), *Org. Geochem.*. Plenum Publications Corp., New York, pp. 419–442.

Lewan, M.D., 1997. Experiments on the role of water in petroleum formation. *Geochim. Cosmochim. Acta* **61**, 3691–3723.

Lewan, M.D., 1998. Sulphur-radical control on petroleum formation rates. *Nature* **391**, 164–166.

Lewan, M.D., 2002. New insights on timing of oil and gas generation in the central Gulf Coast Interior Zone based on hydrous pyrolysis kinetic parameters. *Gulf Coast Assoc. Geol. Soc. Trans.* **52**, 607–620.

Lewan, M.D., Ruble, T.E., 2002. Comparison of petroleum generation kinetics by isothermal hydrous and nonisothermal open-system pyrolysis. *Org. Geochem.* **33**, 1457–1475.

Louis, M.C., Tissot, B.P., 1967. Influence de la temperature et de la pression sur la formation des hydrocarbures dans les argyles a kerogene. *Proc. Seventh World Petrol. Congr.* **2**, 47–60.

Maier, C.G., Zimmerley, S.R., 1924. The chemical dynamics of the transformation of organic matter to bitumen in oil shale. *Bull. Univ. Utah* **14**, 62–81.

Majorowicz, J., Plewa, S., 1979. Study of heat flow in Poland with special regard to tectonophysical problems. In: Čermák, V., Rybach, L. (Eds.), *Terrestrial Heat Flow in Europe*. Springer-Verlag, Berlin, pp. 240–252.

March, J., 1985. *Advanced Organic Chemistry: Reactions, Mechanisms, and Structure*, third ed. John Wiley & Sons, New York, 1346 p.

McKee, R.H., Lyder, E.E., 1921. The thermal decomposition of shales. I-Heat effects. *J. Ind. Eng. Chem.* **13**, 613–618.

Miknis, F.P., Turner, T.F., 1995. The bitumen intermediate in isothermal and nonisothermal decomposition of oil shale. In: Snapr, C. (Ed.), *Composition, Geochemistry and Conversion of Oil Shales*. Kluwer Academic Publishers, Netherlands, pp. 295–311.

Momper, J.A., 1978. Oil migration limitations suggested by geological and geochemical considerations*Physical and Chemical Constraints on Petroleum Migration*, vol. 1. American Association of Petroleum Geologists Short Course, Tulsa, pp. B1–B60.

Nemčok, M., Nemčok, J., Wojtaszek, M., Ludhova, L., Oszczypko, N., Sercombe, W.J., Cieszkowski, M., Paul, Z., Coward, M.P., Ślaczka, A., 2001. Reconstruction of Cretaceous rifts incorporated in the outer west Carpathian wedge by balancing. *Marine and Petroleum Geology* **18**, 39–64.

Orr, W.L., Sinninghe-Damsté, J.S. (1990). Geochemistry of sulfur in petroleum systems. In: Orr, W.L. White, C.M. (Eds.), Geochemistry of Sulfur in Fossil Fuels, American Chemical Society Symposium Series 429, Washington, DC, pp. 2–29.

Oszczypko, N., 1997. The early-middle Miocene Carpathian peripheral foreland basin (Western Carpathians, Poland). *Przegląd Geologiczny* **45**, 1054–1063.

Oszczypko, N., Ślączka, A., 1989. The evolution of the Miocene basin in the Polish Outer Carpathians and their Foreland. *Geologycky Zbornik* **40**, 23–36.

Plewa, S., 1976. The new results of surface heat flow investigations of earth crust performed in Karpaty mountains. *Public Geophysics Polish Academy of Sciences* **A-2** (101), 185–190.

Plewa, M. (1991). The heat flow on Polish territory. *Zeszyty Nauk. Akad. Górn.-Hutn.* (*Acad. Min. Metall. Bull.*) **1373**, Geofizyka Stosowana (*Appl. Geophys.*) **8**, 141–151 (in Polish with Engl. abst.).

Pepper, A.S., Corvi, P.J., 1995. Simple kinetic models of petroleum formation. Part III: Modelling an open system. *Marine and Petroleum Geology* **12**, 417–452.

Reynolds, J.G., Burnham, A.K., Mitchell, T.O., 1995. Kinetic analysis of California petroleum source rocks by programmed temperature micropyrolysis. *Organic Geochemistry* **23**, 109–120.

Ruble, T.E., Lewan, M.D., Philp, R.P., 2001. New insights on the Green River petroleum system in the Uinta basin from hydrous pyrolysis experiments. *American Association of petroleum Geologist Bulletin* **85**, 1333–1371.

Ruble, T.E., Lewan, M.D., Philp, R.P., 2003. Reply to Curry Discussion on "New insights on the Green River petroleum system in the Uinta basin from hydrous pyrolysis experiments". *American Association of Petroleum Geologists Bulletin* **87**, 1535–1541.

Schenk, H.J., Horsfield, B., Kroos, B., Schaefer, R.G., Schwochau, K., 1997. Kinetics of petroleum formation and cracking. In: Welte, D., Horsfield, B., Baker, D. (Eds.), *Petroleum and Basin Evolution*. Springer-Verlag, Berlin, pp. 233–269.

Ślączka, A. (1996). Oil and gas in Nothern Carpathians. In: Wessely, G., Liebl, W. (Eds.), Oil and Gas in Alpidic Thrustbelts and Basins of Central and Eastern Europe. EAGE, *Geol. Soc. London Spec. Publ.* **5**, 187–195.

Ślączka, A., Kamiński, M.A. (1998). A Guidebook to excursions in the Polish Flysch Carpathians: Special Publication No. 6, Grzybowski Foundation, Kraków, 171 p.

Tissot, B., 1969. Premières donneés sur les mécanismes et la cinétique de la formation du pétrole dans les sédiments simulation d'un schéma réactionnel sur ordinateur. *Revue de l'Institut Français du Pétrole* **24**, 470–501.

Tissot, B.P., Welte, D.H., 1984. *Petroleum Formation and Occurrence*, second ed. Springer-Verlag, New York, 699 p.